Available online at www.sciencedirect.com

ScienceDirect

Procedia Structural Integrity 2 (2016) 1530–1537

Structural Integrity Procedia

www.elsevier.com/locate/procedia

21st European Conference on Fracture, ECF21, 20-24 June 2016, Catania, Italy

Magnetoelastic properties in polycrystalline ferromagnetic shape memory Heusler alloys

M. Sofronie*, F. Tolea, A.D. Crisan, B. Popescu, M. Valeanu

National Institute of Materials Physics, Atomistilor Str. No.405A, Magurele,077125, Romania

Abstract

The influence of the heat treatments on the martensitic transformation, magnetic properties and thermo- and magnetic induced strain on $Ni_{50}Fe_{20}Ga_{27}Cu_3$ ferromagnetic shape memory alloy prepared as ribbons by melt–spinning technique are investigated. The degree of atomic order as effect of different thermal treatments produces important changes in the magneto-crystalline anisotropy of the martensite phase. The anomalies evidenced in the thermo-and magnetic- strain curves are discussed and correlated with the thermo-magnetic data. The transformation-induced strains with and without magnetic field have been measured, the results setting out the influence of the pre-martensitic transformation.

Keywords: Ferromagnetic Shape Memory Alloys (FSMA), Martensitic Transformation (MT), Rapid solidification, Magnetic Field Induced Strains (MFIS)

1. Introduction

The so called martensitic transformation (MT), specific to shape memory alloys (SMA), is a thermo-elastic reversible structural phase transition between a high symmetry phase and a lower one. On cooling, the high temperature austenite phase undergoes a diffusionless transformation in which atoms shift cooperatively reducing the symmetry and forming the low temperature martensite phase. Ferromagnetic SMA (FSMA) are materials in which MT appears at temperatures lower than the magnetic transition temperatures. For Heusler type FSMA, the transition takes place between austenite (with B2 or ordered $L2_1$ structure) and either a seven-layer (14 M), a five-

* Corresponding author. Mihaela Sofronie, Tel.: +40-(0)21-3690185; fax: +40-(0)21-3690177.
E-mail address: mihsof@infim.ro

10.1016/j.prostr.2016.06.194

layer modulated (10 M) or a non-modulated (L10 tetragonal) martensite structure, depending on composition and thermal history. The large magnetic field induced strain (MFIS), the high frequency response and the shape memory effect evidenced in FSMA recommend them as promising materials for magnetically controlled actuators.

The MFIS effect is induced by the magnetic field which produces a reorientation of the twin variants (martensitic domains). A large MFIS of about 0.2% was reported for Ni–Mn–Ga single crystals **(**Ullakko K. et al. (1996)) leading to worldwide intensive investigations on this materials system, thus, increasing the understanding level of the physics behind this effect. Further studies have shown that the MFIS values are even higher for martensite with modulated structure; thus, a MFIS of 6 % was reported for the five-layered tetragonal phase (Heczko O. et al (2000)) and of 10% for the seven-layered martensite (Sozinov A. et al (2002)). Ni-Mn-Ga fibers tailored with a bamboo like grains structure, with one dimensional constraint, were reported to have 1% MFIS (Scheerbaum N. et al (2010). Thin films, in which the grains span the thickness of the film, have two dimensional constraints and show up to 0.04% MFIS (Ohtsuka M. et al (2007)). Bulk Ni-Mn-Ga polycrystals highly textured and with large grains have three dimensional constraints and show MFIS of up to 0.3%, (Gaitzsch U. et al (2007)). However, the intrinsic brittleness of Ni_2MnGa is a disadvantage for practical applications. Therefore, the development of new ferromagnetic shape memory alloys with better mechanical properties is strongly looked for. The Ni-Fe-Ga (Sofronie M.et al (2010), Tolea F. et al. (2015)) near stoichiometric Heusler alloys has drawn much attention as an alternative to the brittle Ni-Mn-Ga FSMA (Chernenko V.A. et al (2013), Algarabel P.A. et al (2004), Oikawa K. et al (2002)).

Recently, a thermoelastic MT in the ferromagnetic state, associated with a shape memory effect, was evidenced in Ni–Fe–Ga Heusler type alloy (Oikawa K. et al (2002)). For the stoichiometric Ni_2FeGa, the MT temperature is around 145 K, the system being ferromagnetic up to 430 K. For the off-stoichiometric compounds, the martensitic transition shifts to higher temperatures with increasing Ni content. Several studies have been focused on the influence of thermal history, (Imano Y. et al (2006), Santamarta R. et al (2006)) iron concentration (Liu Z. H. et al (2004)) and trace elements (Zheng H. X. et al (2005)) on the MT in Ni–Fe–Ga alloy. Cobalt is one of the most studied substitution element in Ni–Fe–Ga alloys. Besides its well known effect in increasing the Curie temperature, cobalt may increase or decrease the MT temperature, depending on the element which is partially substituted. However, the mechanical properties of the alloy are unexpectedly enhanced (Sui J. H. et al (2008), Picornell C. et al (2008), Chernenko V. A. et al (2009)). A MFIS of about 0.7% at 300K is found in $Ni_{52}Fe_{18}Ga_{27}Co_3$ (Morito H. et al (2005)), smaller than the 10% strain of Ni-Mn-Ga (Sozinov A. et al (2002)) because the magnetocrystalline anisotropy constant is still low in Ni-Fe-Ga-Co. However, the practical advantage of Ni–Fe–Ga alloys over the other mentioned compounds is related to its better ductility which was associated to a secondary phase. While the stoichiometric Ni_2FeGa compound is located in the $\beta+\gamma$ two phase zone (Oikawa K. et al (2007)), the improved ductility of Ni-Fe-Ga based alloys was attributed to the precipitation of the secondary γ phase, with face centered cubic (fcc) type structure, situated at the grain boundaries and which might favor the cohesion between grains (Santamarta R.et al (2006)). Although a low percentage of secondary γ phase would have beneficial effects on the mechanical properties, a high quantity of this phase might reduce the relative amount of transformable phase and hence the shape memory properties. It is not trivial to engineer such a material with an optimal control of both the active and secondary γ phase. It was reported that TTs performed at high temperatures or the alloying with some additional elements may favor the precipitation of the γ phase.

Recently reported data have shown that suitable quenching preparation techniques, like melt spinning, may prevent the formation of the secondary γ phase even for the Ni-Fe-Ga based alloys with relative low Ga content (<27at%) (Liu Z.H.et al (2003), Okumura H. et al (2010)). Rapidly quenched ribbons as well as thin films with tailored MT and Curie temperatures may offer new opportunities for applications as miniaturized active elements for sensors, actuators and other functional devices.

In this work, the Ni-Fe-Ga alloys doped with non-magnetic Cu are investigated. The melt spun ribbons high texture is turned to practical account in addition to the enhanced mobility of martensitic twin variant boundaries promoted by the quenched strains in order to study the thermo- and magnetic-strain behavior of the melt-spun $Ni_{50}Fe_{20}Ga_{27}Cu_3$ ribbons.

2. Experimental

The polycrystalline sample $Ni_{50}Fe_{20}Ga_{27}Cu_3$ was prepared from high-purity elements by arc melting in argon atmosphere. The resulted ingot was inductively melted in a quartz tube in an argon atmosphere and then rapidly quenched by the melt spinning technique. As-prepared (AP) ribbons of about 20 μm thickness and 2 mm width were obtained by evacuating the melt on a rotating copper wheel (linear velocity of 20 m/s, 50 kPa Ar overpressure and crucible with nozzle diameter of 0.5 mm).

The as prepared ribbons were subjected to two different thermal treatments (TTs): 20 minutes at 400ºC (TT1) and 800ºC (TT2) followed by slow cooling. The crystalline structure was investigated by X-ray diffraction using a Bruker D8 Advance diffractometer (Cu Kα radiation). The microstructure was investigated by Scanning Electron Microscopy (SEM) via a Zeiss Evo 50XVP microscope. The ribbons composition, verified by energy dispersive X-ray spectroscopy, was the nominal one, within the limits of the method accuracy. The MT temperatures were determined by differential scanning calorimetry (DSC) via a Netzsch Differential Scanning Calorimeter with a scanning rate of 20 K/min. The start and finish temperatures for the direct (Ms, Mf) and reverse (As, Af) transformations were determined from the DSC thermograms by the tangential method (Gmelin E. et al (1995)). Magnetic measurements below 400 K were performed with a SQUID (Quantum Design) magnetometer in fields up to 5T. The linear thermal expansion (LTE) and magnetostrictive measurements have been performed by means of two strain gauges, one was glued on the ribbon length and the other serving as reference and in-plane strains, with the field applied either parallel or transversal to the ribbon plane were recorded as function of temperature and magnetic field. The "Vishay Micro-Mesurements Model P3 strain indicator and recorder" and the magnetic platform Cryogenic Ltd. in the temperature range from 120 to 300 K and fields up to 5 T were used for completing these measurements.

3. Results and discussion

3.1. Calorimetry data

DSC scans were performed on all samples over a temperature range between 120 K and 200 K in order to observe the MT. Fig.1 shows DSC curves of the as prepared (AP) ribbons and after the thermal treatments (TT1 and TT2). For the AP ribbons the martensite start temperature is 149K very close to that of the stoichiometric Ni_2FeGa ribbons (142 K) (Liu Z.H.et al (2003)). The TT at 400ºC brings no significant changes in the MT characteristic temperatures. As an effect of TT2, the MT shifts at slightly higher temperatures and the heat of transformation slowly decreases but the range of MT (Af-Mf) is enlarged suggesting the structure degradation. The temperatures corresponding to the peak maxima in the direct - austenite to martensite -T_{Mp} and reverse - martensite to austenite - T_{Ap} are presented in Table 1.

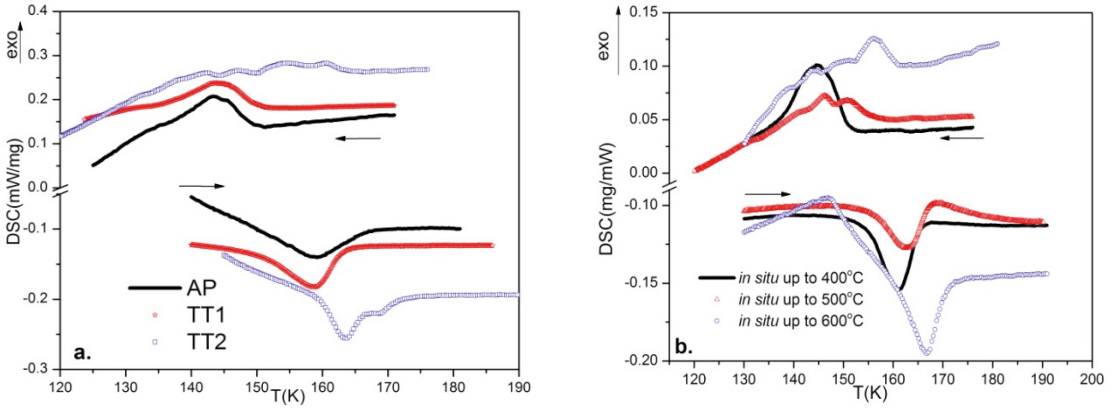

Fig. 1 DSC measurements on as-prepared (AP) and thermally treated ribbons (TT1 and TT2)(a); In situ DSC scans on AP ribbons at different temperatures (b).

Table 1. The average transformation heat (calculated as average between the direct and reverse transformation) for as prepared (AP) and after different TTs, the temperatures corresponding to the peak maxima in the direct - austenite to martensite -T_{Mp} and reverse - martensite to austenite - T_{Ap} , the range of martensitic transformation (Af-Mf) and Curie temperatures (T_C)

Samples	T_{Mp} (K)	T_{Ap} (K)	Q (J/g)	A_f-M_f (K)	T_C (K)
AP	143	156	1.6	25	316
TT1	144	158	1.5	26	323
TT2	154	163	1.2	37	321

In order to find the optimal TT the AP ribbons were subjected to *in situ* successive calorimetric scans around MT at temperatures progressively increasing from 400ºC to 600ºC, each scan simulating the effect of a thermal treatment (Tolea F. et al (2015)). The results confirm the rise of the MT temperatures by increasing the treatment temperature but the multi-peaks transformation, for T > 500ºC, suggests the alloy structural degradation. However, the diffraction data collected on ribbons after TT2 indicates a higher atomic order proved by $L2_1$ structure.

3.2. Structure and morphology

Room temperature XRD measurements (Fig.2.a) were recorded for the as prepared ribbons (AP) as well as after different TTs (TT1 and TT2).

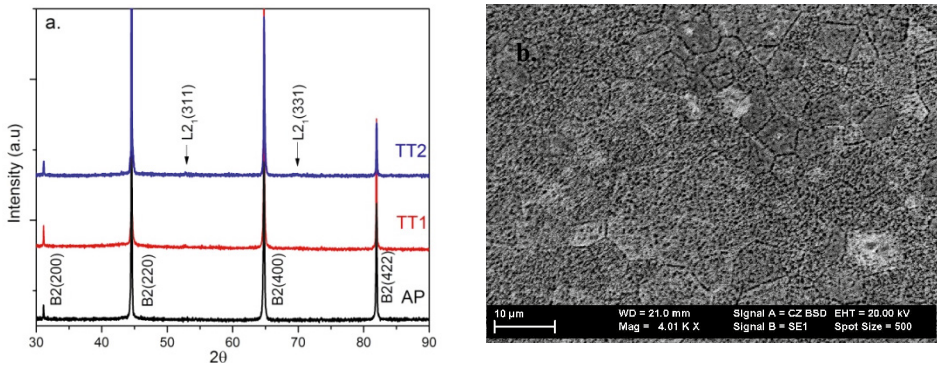

Fig. 2 The X-ray diffraction patterns recorded at room temperature for the as-prepared (AP) and thermally treated ribbons (TT1 and TT2)(a); SEM image for TT2 sample (b)

The XRD patterns for AP sample show that the compound crystallizes in the B2 cubic structure, a partial disordered Heusler-type structure (Tolea F. et al (2015)). As expected, the ribbons are highly textured proved by the enhanced intensity of the (400) reflection. This texture is the result of the different cooling velocity of the contact side (with the wheel surface) and the free side of the ribbons (Okumura H. et al (2010), Wang J. et al (2013), Sofronie M.et al (2015)). The improved atomic ordering in ribbons after TT2 is proved by the two small peaks in the XRD pattern, indexed as (311) and (331) reflections specific to the $L2_1$ structure and without any trace of the secondary γ phase. Whoever, SEM image (Fig.2.b) reveals the microstructure degradation of TT2 ribbons, with high density of cracks and voids. These give an aspect of porous material (Tolea F. et al (2015)) and induce the brittleness of the ribbons.

3.3. Magnetic and Magnetoelastic properties

Fig 3 shows the thermo-magnetic curves of as prepared and TT ribbons measured at 200 Oe during field-cooling followed by field-heating as indicated by the arrows. The measurements were done in plane, with the field along the ribbon direction. The abrupt decrease in the magnetization near 325K marks the magnetic order-disorder transition. As can be seen the Curie temperatures- taken as the temperatures where dM/dT=0 - are slightly increasing (~ 10K) as an effect of the thermal treatments. The magnetic hysteresis observed on the three curves in the vicinity of 150K

is the signature of the martensite transformation as a first-order phase transition. The values of the MT characteristic temperatures are in agreement with those obtained by DSC measurements.

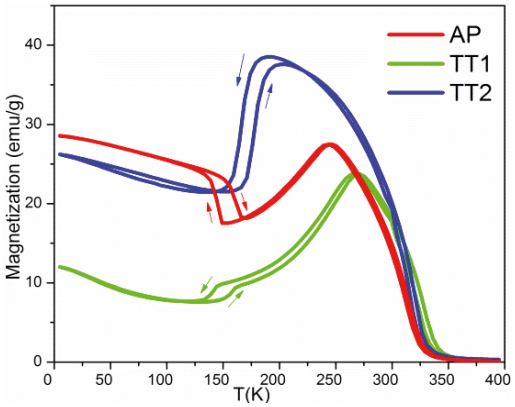

Fig. 3 Thermomagnetic measurements at 200 Oe of as prepared (AP) and thermally treated at 400°C (TT1) and 800°C (TT2) ribbons

To be noted that the low-field curves are very sensitive to the magnetic anisotropy of the samples. Generally, by cooling, magnetization shows a marked decrease in the transition from the cubic austenite (low anisotropy) to the martensite with lower structural symmetry (high anisotropy). This behaviour may be observed on the thermally treated ribbons (TT1 and TT2). However, comparing the M(T) curves in Fig.3, two distinctive features are emerging. First, for the as prepared and thermally treated at 400°C (TT_1) ribbons, the austenite magnetization increases between Af and T_C giving rise to a Hopkinson peak at T_C. Such behaviour was already reported on near stoichiometric Ni_2MnGa (Wang J.et al (2009), Albertini F. et al (2002)) and Ni_2FeGa (Qian J.F. et al (2011)) rapidly quenched or annealed at low temperatures ribbons, but is absent for ribbons with high atomic order annealed at high temperatures (e.g. ribbons at TT2) or on bulk samples with the same composition. The Hopkinson peak was previously observed in soft magnetic materials and its origin was associated to the reduction of the anisotropy constant when the temperature increases and approaches the Curie point. For Heusler type FSMA, the large magnetization decrease between T_C and Ms may be caused by a pre-martensite transformation that enhances the magnetic anisotropy.

The second feature consists of the surprising increase of the magnetization when proceeding from austenite to martensite for the as prepared ribbons. In addition, the highest magnetization value measured in low field at 5K is obtained on the as prepared ribbons. These two observations suggest that the as prepared ribbons in the martensite state have the lowest magnetic anisotropy. From this point of view the highest magnetic anisotropy in martensite state is shown by TT1 ribbons followed by TT2 ribbons and last by the as prepared ones. Concerning the as prepared ribbons, we may consider that the structural distortion in systems with high atomic disorder could induce actually an amorphous state with soft magnetic behaviour.

The relative length changes $\Delta l/l$ referenced to 300K in zero and 5T magnetic field applied along and transversal to the ribbons, during the cooling/heating process at temperatures ranging from 120 K to 300 K are shown in Fig 4. In ZFC, and passing through the MT, the ribbons undergo a continuous contraction as a result of the tendency of the variants to accommodate the strain in order to minimize the elastic energy and to maintain the shape of the ribbons without preferred direction of growth for the variants (Tolea. F, Tolea M. (2015)). The more pronounced contraction in the range of transformation infers a tetragonal structure in the martensite state with $c/a<1$ (Chen F.et al (2006)). The largest spontaneous strain is observed on the as prepared ribbons with the highest atomic disorder whereas for the TT2 ribbons, the strain associated to the MT is the lowest. In the last situation, it could be supposed that the voids observed by SEM may accommodate the local strains. By heating, the deformation is completely recovered via expansion, the ribbons showing a good thermo-elastic transformation (Fig.4.a). The LTE measurements performed in transversal mode reveal a lower contraction that may be assigned to the ribbon texture with the grains oriented along the spinning direction.

Under applied magnetic field in the austenite state by cooling and passing through MT, the martensite variants

nucleate and grow along the field direction, in order to minimize the Zeeman energy. This nucleation mechanism does not depend on the mobility of the martensitic variants (Aksoy S. et al (2007)) but may be affected by the existence of cracks within or at the grain boundaries. The variants with the easy magnetic axis along the applied field direction grow at the expense of others, giving rise to a largest strain in the field direction (MFIS).

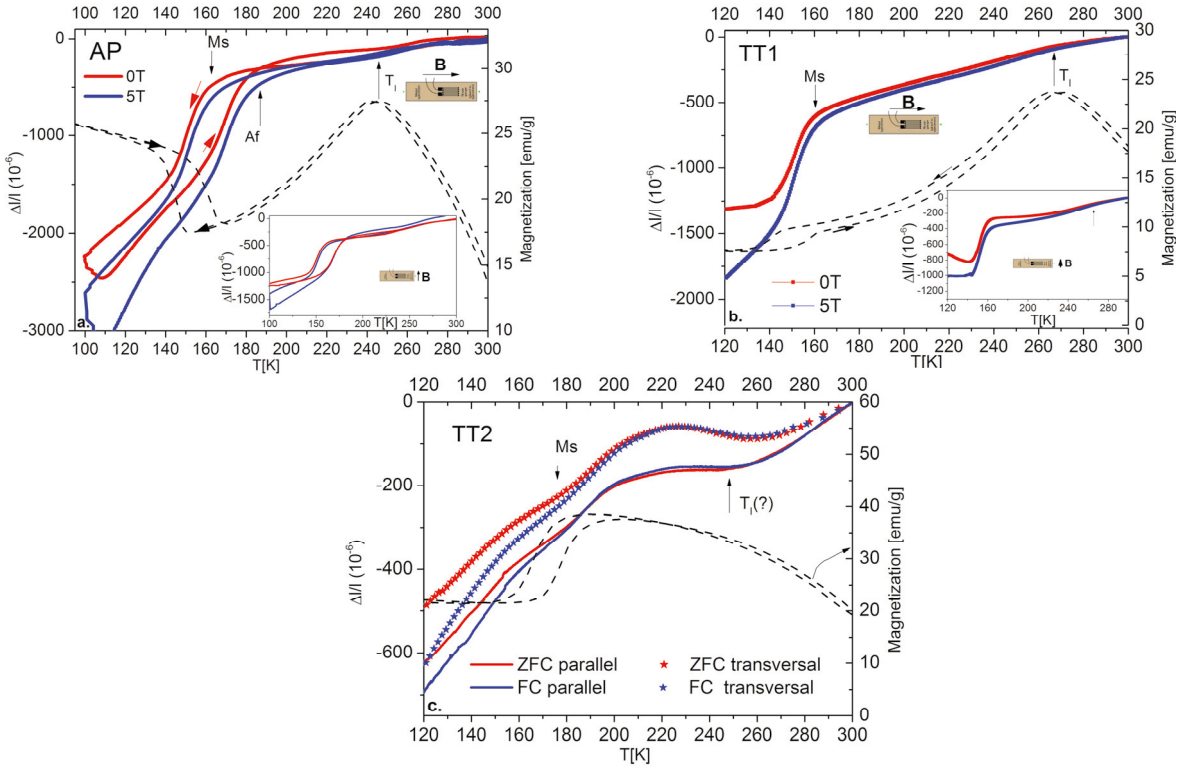

Fig.4 The temperature dependence of parallel and transversal (in Insets for AP and TT1 samples) strain under zero and 5T as well as the low-field thermo-magnetic curves for as prepared (a) thermal treated at 400ºC - TT1 (b) and at 800ºC - TT2 (c) ribbons. T_I marks the pre-martensite start temperature

All the anomalies evidenced in the thermo-magnetic data have a correspondence in the thermo-strain curves. Thus, the martensitic characteristic temperatures marked by slope changes in the thermo-strain curves and evaluated by tangential method are ~10K higher than those given by DSC for the as prepared and TT1 ribbons but are in good agreement with those for TT2 ribbons. Further, a similar slope change is evidenced at the temperature of the Hopkins peak and may be assigned to the start of the pre-martensite transformation (T_I). However surprisingly, the thermo-strain curves for TT2 ribbons measured in zero field as well as in 5T reveal a similar pre-martensite transformation that was not detected in the thermo-magnetic measurements. It is to noted that, the divergence between the ZFC and FC thermo-strain curves starts at T_I for the as prepared and TT1 ribbons, but only at Ms for TT2 ribbons. The effect of the magnetic field in the temperature range of interest can be seen more clearly by calculating the magnetic field induced strain (MFIS) as the difference between the thermo-strain at 5T and at zero field. Fig.5.a shows MFIS for the under discussion ribbons calculated at cooling for the parallel configuration and the arrows indicate the start martensite temperatures obtained from DSC. The ribbons with lower atomic order – as prepared and TT1 ribbons- show higher MFIS values. Although MFIS in TT2 ribbons has relative low values, they seem to reflect the variants nucleation along the field direction even though the sample contraction persists below the martensite finish temperature.

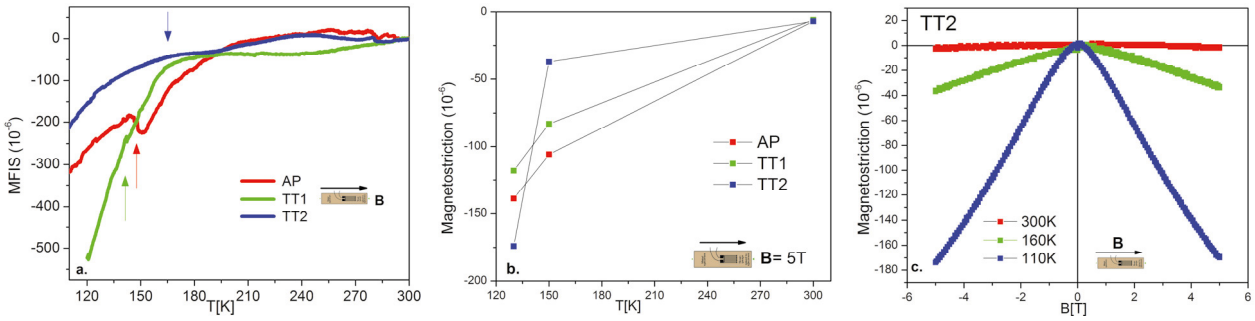

Fig.5. MFIS values for the three types of ribbons calculated at cooling for parallel configuration; the arrows indicate the start martensite temperatures(a), Temperature dependence of magnetostriction at 5T for all samples (b), Parallel magnetostriction curves of TT2 ribbons as a function of the field at different temperatures(c);

Isothermal magnetostriction measurements (Fig.5.b) in magnetic fields up to 5T, applied parallel to the measuring direction, were performed at different temperatures, specific to the each sample. At room temperature, all the samples show a same negative magnetostriction (-7 $x10^{-6}$) but increase in the temperature range of the MT. It is to note that highest magnetostriction at the MT finish is obtained for TT2 (Fig.5.c) ribbons and the value is close to the MFIS value at the same temperature.

Conclusions

Single phase $Ni_{50}Fe_{20}Ga_{27}Cu_3$ ribbons with high atomic disorder have been obtained by melt–spinning. The effect of different heat treatments on the MT and the MFIS was studied via magnetometry and thermal-strain measurements in zero and 5T magnetic field. The thermal treatments bring no important changes in the martensite transformation characteristic temperatures but hardly increase the magnetocrystalline anisotropy in the martensite phase. The largest MFIS is observed on the as prepared ribbons with the highest atomic disorder whereas for the ribbons with high atomic order the magnetic strain associated to the MT is the lowest. The twin boundaries are pinned by the cracks and voids which appear alongside the atomic ordering and lead to the decrease of the MFIS for the ribbons treated at higher temperature.

Aknowledgement

This work was supported by a grant of the Romanian Ministry of Education, CNCS – UEFISCDI, project number PN-II-ID-PCE-2012-4-0516 and by the CORE PROGRAM 2016-2017.

References

Ullakko K., Huang J. K., Kantner C., O'Handley R. C., Kokorin V. V. 1996 Large magnetic-field-induced strains in Ni_2MnGa single crystals, Appl. Phys. Lett. 69, 1966-1968.

Heczko O., Sozinov A, Ullakko K., 2000, Giant field-induced reversible strain in magnetic shape memory NiMnGa alloy, IEEE Trans. Magn., 36, 5, 3266-3268.

Sozinov A., Likhachev A. A., Lanska N., Ullakko K., 2002,Giant Magnetic-Field-Induced Strain in NiMnGa Seven Layered Martensitic Phase, Applied Physics Letters, 80, 10, 1746-1748.

Scheerbaum N., Heczko O., Liu J., Hinz D, Schultz L., Gutfleisch O., 2008, Magnetic field-induced twin boundary motion in polycrystalline Ni–Mn–Ga fibres, New Journal of Physics, 10,1-8.

Ohtsuka M., Matsumoto M., Koike K., Takagi T., Itagaki K., 2007, Martensitic transformation and shape memory effect of Ni-rich Ni2MnGa sputtered films under magnetic field, Journal of Magnetism and Magnetic Materials, 310, 2782-2784.

Gaitzsch U., Potschke M., Roth S., Rellinghaus B., Schultz L., 2007 Mechanical training of polycrystalline 7 M $Ni_{50}Mn_{30}Ga_{20}$ magnetic shape memory alloy, Scripta Materialia, 57, 493-495.

Sofronie M., Tolea F., Kuncser V., Valeanu M., 2010, Martensitic transformation and accompanying magnetic changes in Ni–Fe–Ga–Co alloys, J. Appl. Phys. 107, 113905-113905-5.

Tolea F., Sofronie M., Crisan A.D., Enculescu M., Kuncser V., Valeanu M., 2015, Effect of thermal treatments on the structural and magnetic transitions in melt-spun Ni-Fe-Ga-(Co) ribbons, J. All. Comp., 650, 664-670.

Chernenko V.A., Barandiarán J.M., L'vov V.A., Gutiérrez J., Lázpita P., Orue I., 2013, Temperature dependent magnetostrains in

polycrystalline magnetic shape memory Heusler alloys, J. All. Comp.,577, S1, S305–S308.
Algarabel P.A., Magen C., Morellon L., Ibarra M.R., Albertini F., Magnani N., Paoluzi A., Pareti L., Pasquale M., Besseghini S., 2004, Magnetic-field-induced strain in Ni2MnGa melt-spun ribbons. J. Magn. Magn. Mat. 272-276, 2047-2048.
Oikawa K., Ota T., Ohmori T., Tanaka Y., Morito H., Fujita A., Kainuma R., Fukamichi K., Ishida K., 2002, Magnetic and martensitic phase transition in ferromagnetic Ni-Fe-Ga shape memory alloys, Appl. Phys. Lett. 81, 5201-5203.
Imano Y., Omori T., Oikawa K., Sutou Y., Kainuma R., Ishida K., 2006, Martensitic and magnetic transformations of Ni–Ga–Fe–Co ferromagnetic shape memory alloys, Mater. Sci. Eng., A 970, 438–440.
Santamarta R, Cesari E, Font J, Muntasell J, Pons J, Dutkiewicz J, 2006, Effect of atomic order on the martensitic transformation of Ni-Fe-Ga alloys, Scr. Mater. 54 1985-1989.
Liu Z. H., Liu H., Zhang X. X., Zang M., Dai X. F., Hu H. N., Chen J. L., Wu G. H., 2004, Martensitic transformation and magnetic properties of Heusler alloy Ni–Fe–Ga ribbon, Phys. Lett. A 329, 214.
Zheng H. X., Liu J., Xia M. X., Li J. G., 2005, Martensitic transformation of Ni–Fe–Ga–(Co, Ag) magnetic shape memory alloys, J. Alloys Compd. 387, 265-268.
Sui J. H., Gao Z., Yu H., Zhang Z., Cai W., 2008, Martensitic and magnetic transformations of $Ni_{56}Fe_{17}Ga_{27-x}Co_x$ high temperature ferromagnetic shape memory alloys, Scr. Mater. 59, 874-877.
Picornell C., Pons J., Cesari E., Dutkiewicz J., 2008, Thermal characteristics of Ni–Fe–Ga–Mn and Ni–Fe–Ga–Co ferromagnetic shape memory alloys, Intermetallics 16, 751-757.
Chernenko V. A., Oikawa K., Cheielus M., Besseghini S.,. Villa E,. Albertini F, Roghi L., Paoluzi A., Mullner P., Kainuma R., Ishida K., 2009, Properties of Co-alloyed Ni-Fe-Ga ferromagnetic shape memory alloys, J. Mater. Eng. Perform. 18, 548-553.
Morito, H. Oikawa K., Fujita A., Fukamichi K., Kainuma R., Ishida K., 2005, Enhancement of magnetic-field-induced strain in Ni–Fe–Ga–Co Heusler alloy,Scr. Mater. 53, 1237-1240
Liu Z.H., Zhang M., Cui Y.T., Zhou Y.Q., Wang W.H., Wu G.H., Zhang X.X., Xiao G., 2003, Martensitic transformation and shape memory effect in ferromagnetic Heusler alloy Ni2FeGa, Appl. Phys. Lett. 82, 424–426.
Okumura H. and Uemura K., 2010, Influence of quenching rate on the magnetic and martensitic properties of Ni-Fe-Ga melt-spun ribbons, 108, 3910-043910.
Gmelin E., Sarge St.M., 1995, Calibration of differential scanning calorimeters, Pure & Appl. Chem. 67, 1789-1800.
Wang J., Jiang C., Tachapiesancharoenkij R., Bono D., Allen S.M., O'Handley R.C., 2013, Microstructure and magnetic properties of melt spinning Ni-Mn-Ga, Intermetallics 32, 151-155.
Sofronie M., Tolea F., Kuncser V., Valeanu M., Filoti G., 2015,Magneto-structural properties and magnetic behavior of Fe-Pd ribbons, IEEE Trans. Mag. 51, 2500404.
Wang J., Jiang C., Techapiesancharoenkij R., Bono D., Allen S. M., O'Handley R. C., 2009, Anomalous magnetizations in melt spinning Ni–Mn–Ga, J.Appl. Phys., 106, 023923.
Albertini F., Besseghini S., Paoluzi A., Pareti L., Pasquale M., Passaretti F., Sasso C.P., Stantero A., Villa E.,2002,Structural, magnetic and anisotropic properties of Ni_2MnGa melt-spun ribbons, J. Magn. Magn. Mat.242-245, 1421-1424.
Qian J.F., Liu E.K., Feng L., Zhu W., Li G.J., Wang W.H., Wu G.H., Du Z. W. Fu X., 2011, Unusual magnetic anisotropy in the ferromagnetic shape-,memory alloy Ni50Fe23Ga27, Appl. Phys. Lett. 99, 252504.
Chen F., Menga X.L., Caia W., Zhaoa L.C., G.H. Wub, 2006, Martensitic transformation and shape memory effect of a Ni–Fe–Ga polycrystalline alloy, J. Magn. Magn. Mat 302, 459–462.
Tolea. F, Tolea M., M. Sofronie, M. Valeanu, 2015, Distribution of plates' sizes tell the thermal history in a simulated martensitic-like phase transition, Solid StateCommunications, 213-214, 37–41.
Aksoy S., Krenke T., Acet M., Wassermann E. F., Moya X., Manosa L., Plates A., 2007, Magnetization easy axis in martensitic Heusler alloys estimated by strain measurements under magnetic field, Appl. Phys. Lett. 91,251915.